New Journal of Physics
The open-access journal for physics

Diffraction by a grating made of a uniaxial dielectric–magnetic medium exhibiting negative refraction

Ricardo A Depine[1,4] **and Akhlesh Lakhtakia**[2,3]

[1] Grupo de Electromagnetismo Aplicado, Departamento de Física, Facultad de Ciencias Exactas y Naturales, Universidad de Buenos Aires, Ciudad Universitaria, Pabellón I, 1428 Buenos Aires, Argentina
[2] CATMAS—Computational and Theoretical Materials Sciences Group, Department of Engineering Science and Mechanics, Pennsylvania State University, University Park, PA 16802–6812, USA
[3] Department of Physics, Imperial College, London SW7 2BZ, UK
E-mail: rdep@df.uba.ar

New Journal of Physics **7** (2005) 158
Received 11 January 2005
Published 8 August 2005
Online at http://www.njp.org/
doi:10.1088/1367-2630/7/1/158

Abstract. Diffraction of linearly polarized plane electromagnetic waves at the periodically corrugated boundary of vacuum and a linear, homogeneous, uniaxial, dielectric–magnetic medium is formulated as a boundary-value problem and solved using the Rayleigh method. The focus is on situations where the diffracted fields maintain the same polarization state as the s- or p-polarized incident plane wave. Attention is paid to two classes of diffracting media: those with negative definite permittivity and permeability tensors, and those with indefinite permittivity and permeability tensors. For the situations investigated, whereas the dispersion equations in the diffracting medium turn out to be elliptic for the first class of diffracting media, they are hyperbolic for the second class. Examples are reported with the first class of diffracting media of instances when the grating acts either as a positively refracting interface or as a negatively refracting interface. For the second class of diffracting media, hyperbolic dispersion equations imply the possibility of an infinite number of refraction channels.

[4] Author to whom any correspondence should be addressed.

PII: S1367-2630(05)92834-6

Contents

1. Introduction **2**
2. Grating theory **4**
2.1. Boundary-value problem 4
2.2. Rayleigh method 5
3. Numerical results and discussion **7**
3.1. Classification of constitutive tensors 7
3.2. Cases chosen for investigation 7
3.3. Case I 8
3.4. Case II 11
3.4.1. Cases IIA and IIB 12
3.4.2. Cases IIC and IID 16
4. Concluding remarks **21**
Acknowledgments **21**
References **21**

1. Introduction

Originating primarily from a theoretical speculation of Veselago [1], intensive studies of the propagation of plane electromagnetic waves in isotropic, homogeneous materials with negative real permittivity and permeability scalars have been recently reported [2]–[4]. Materials with these constitutive properties are characterized by a negative index of refraction, because the phase velocity vector is in the opposite direction of the energy flux. This leads to the apparent (but not actual) reversal of the law often attributed to van Snel (but discovered 6 centuries earlier by Ibn Sahl [5]) and to other phenomenons not observed in isotropic materials with positive real permittivity and permeability scalars, such as reversal of both the Doppler shift and Cerenkov radiation, or a change from radiation pressure to radiation tension [1]. Although materials with these characteristics do not seem to occur naturally, composite materials having an effectively negative index of refraction in the microwave range have been constructed [6]–[8], the negative real permittivity and permeability scalars respectively arising from arrays of conducting wires [9] and arrays of split ring resonators [10]. The size and spacing of the array elements being much smaller than the electromagnetic wavelengths of interest, such non-homogeneous composite materials—often called metamaterials—perform as effectively homogeneous materials. As McCall *et al* [11] and Boardman *et al* [12] have pointed out, it is best to call these materials negative-phase-velocity (NPV) materials. This definition has been extended by Mackay and Lakhtakia [13] to encompass the negative projection of the phase velocity vector on the time-averaged Poynting vector (i.e. the direction of energy flux).

Negative refraction by natural crystals has also been observed [14], but that cannot be ascribed to a negative index of refraction; instead, due to anisotropy, the phase velocity vector and the direction of energy flux can sometimes be counterposed [15] to show negative refraction. Counterposition means that the two vectors lie on opposite sides of the normal to a refracting interface. Our focus in this paper is not on such anisotropic materials, but on anisotropic NPV metamaterials.

This focus comes from the fact that the NPV metamaterials synthesized thus far are actually anisotropic in nature, and any hypothesis about their isotropic behaviour holds only under some restrictions on propagation direction and polarization state. As an example, Parazzoli *et al* [7] demonstrated negative refraction using s-polarized microwaves and samples for which the permittivity and permeability tensors have certain eigenvalues that are negative real. Since the use of anisotropic NPV materials offers flexibility in design and ease of fabrication, attention has begun to be drawn to such materials [13], [16]–[19].

The intrinsic difference between NPV and positive-phase-velocity (PPV) materials is easily manifested in simple boundary-value problems. Consider, for example, the reflection and refraction of a plane wave due to a flat boundary between vacuum and an isotropic, homogeneous medium characterized by relative permittivity scalar ϵ and relative permeability scalar μ. The incident plane wave is directed at an angle θ_0 with respect to the normal to the boundary. A simultaneous change in the signs of the real parts of both ϵ and μ changes the phase of the reflection coefficient but not its magnitude [20]; therefore, the reflectance of the boundary is the same for both cases. Consistently with that conclusion, it has been shown that, when the boundary is periodically corrugated, the NPV to PPV (or the PPV to NPV) transformation affects mainly the non-specular reflectances and refractances when the corrugations are shallow, and that the effect on the specular reflectance and refractance intensifies as the corrugation deepens [21]–[23].

Gratings made of homogeneous NPV materials require investigation for two reasons. Firstly, the emergence of these metamaterials promises new types of gratings which could be significantly different from their PPV counterparts. Secondly, all experimental realizations of NPV metamaterials thus far are as periodically patterned composite materials, with the unit cell size smaller, although not extremely, than the wavelength. Due to this finite electrical size of the unit cell, the exposed surface of the metametarial is not planar, but periodically modulated instead. As a result of the grating formation, the specular reflected/refracted waves can be accompanied by non-specular diffracted waves, as has been reported recently [8, 24, 25].

In this paper, we discuss the characteristics of diffraction of plane waves due to the periodically corrugated boundary of vacuum and a linear, homogeneous, uniaxial, dielectric–magnetic NPV medium [13], whose permittivity and permeability tensors share a common distinguished axis which is usually referred to as the optic axis. Thus, four constitutive scalars are needed to characterize the diffracting medium: $\epsilon_{\parallel}$ and $\mu_{\parallel}$, which are the respective elements of the relative permittivity and relative permeability tensors along the optics axis; and $\epsilon_{\perp}$ and $\mu_{\perp}$, which are the elements of the two tensors in the plane perpendicular to the optic axis. These scalars have positive real parts for natural crystals, but their real parts can have any sign for metamaterials. The dispersion equation for harmonic plane waves in such a medium can be factorized into two terms, leading to the conclusion that the medium supports the propagation of two different types of linearly polarized waves, called magnetic and electric modes [26, 27].

The plan of this paper is as follows. Section 2 contains a description of the boundary-value problem for the diffraction of a plane wave by a grating made of the chosen anisotropic NPV medium, as well as a description of the Rayleigh method adopted to solve the problem numerically. Section 3 is devoted to a discussion of numerical results for two important classes of the NPV medium: either both the relative permittivity and the relative permeability tensors are negative definite (section 3.3) or both are indefinite (section 3.4). For the first class, the dispersion equation has the same algebraic form as ellipses in plane geometry; but it is isomorphic to hyperbolas for the second case. The incident plane wave is linearly polarized, and the incidence plane as well as the orientation of the optic axis are chosen such that the reflected and the

refracted waves are of the same polarization state as the incident plane wave. Most importantly, we show that refraction can possibly occur in terms of an infinite number of propagating (i.e., non-evanescent) plane waves for certain types of NPV gratings. Concluding remarks are provided in section 4. Let us point out here that, to our knowledge, this is the first report on diffraction by gratings made of anisotropic NPV materials.

An $\exp(-\mathrm{i}\omega t)$ time-dependence is implicit, with ω as angular frequency, t as time and $\mathrm{i} = \sqrt{-1}$. A cartesian coordinate system $\vec{r} = (x, y, z)$ is used.

2. Grating theory

2.1. Boundary-value problem

Let us consider the periodically corrugated boundary $y = g(x) = g(x + d)$ between vacuum and a linear, homogeneous, uniaxial dielectric–magnetic medium, with d being the corrugation period. The region $y > g(x)$ is vacuous, whereas the medium occupying the region $y < g(x)$ is characterized by complex-valued relative permittivity and relative permeability tensors denoted by $\tilde{\epsilon}$ and $\tilde{\mu}$, respectively. In dyadic form [28], these tensors can be written as

$$\tilde{\epsilon} = \epsilon_\perp \tilde{I} + (\epsilon_\parallel - \epsilon_\perp)\hat{c}\hat{c}, \tag{1}$$

$$\tilde{\mu} = \mu_\perp \tilde{I} + (\mu_\parallel - \mu_\perp)\hat{c}\hat{c}, \tag{2}$$

where $\tilde{I}$ is the identity dyadic and the unit vector $\hat{c} = (c_x, c_y, c_z)$ is parallel to the optic axis of the medium.

A linearly polarized electromagnetic plane wave is incident on the boundary from the vacuous region $y > g(x)$ at an angle θ_0 ($|\theta_0| < \pi/2$), with respect to the y axis, the plane of incidence being the xy plane. In the vacuous half-space $y > \max\, g(x)$, the electromagnetic field is rigorously represented by the following Floquet expansions:

$$\vec{E}_1 = \left[\frac{\beta_0^{(1)}}{k_0} H_0 \hat{x} + \frac{\alpha_0}{k_0} H_0 \hat{y} + E_0 \hat{z}\right] \exp\left[\mathrm{i}(\alpha_0 x - \beta_0^{(1)} y)\right] + \sum_{n=-\infty}^{+\infty} \left[-\frac{\beta_n^{(1)}}{k_0} S_n \hat{x} + \frac{\alpha_n}{k_0} S_n \hat{y} + R_n \hat{z}\right] \exp\left[\mathrm{i}(\alpha_n x + \beta_n^{(1)} y)\right], \tag{3}$$

$$\vec{H}_1 = \left[-\frac{\beta_0^{(1)}}{k_0} E_0 \hat{x} + \frac{\alpha_n}{k_0} E_0 \hat{y} + H_0 \hat{z}\right] \exp\left[\mathrm{i}(\alpha_0 x - \beta_0^{(1)} y)\right] + \sum_{n=-\infty}^{+\infty} \left[\frac{\beta_n^{(1)}}{k_0} R_n \hat{x} - \frac{\alpha_n}{k_0} R_n \hat{y} + S_n \hat{z}\right] \exp\left[\mathrm{i}(\alpha_n x + \beta_n^{(1)} y)\right]. \tag{4}$$

Here and hereafter, $\hat{x}$, $\hat{y}$ and $\hat{z}$ are the unit Cartesian vectors; $k_0 = \omega/c$ is the wavenumber in vacuum and c the speed of light in vacuum; E_0 and H_0 are complex amplitudes depending on the polarization of the incident plane wave; R_n and S_n, $|n| \geqslant 0$, are scalar coefficients to be determined by solving the boundary-value problem; and

$$\alpha_0 = k_0 \sin\theta_0, \qquad \alpha_n = \alpha_0 + 2n\pi/d, \qquad \beta_n^{(1)} = +\sqrt{k_0^2 - \alpha_n^2}. \tag{5}$$

We note that for any n, either $\beta_n^{(1)}$ is real and positive, or it is imaginary and positive.

In the diffracting medium, for plane waves with electric-field amplitude vector $\vec{e}$ and wavevector $\vec{k}$, the Maxwell equations yield the condition [26]

$$\tilde{W} \cdot \vec{e} = \vec{0}, \tag{6}$$

where $\vec{0}$ is the null vector and the dyadic

$$\tilde{W} = (\vec{k} \times \tilde{\mu}^{-1}) \cdot (\vec{k} \times \tilde{I}) + k_0^2 \tilde{\epsilon}. \tag{7}$$

The dispersion equation

$$(\vec{k} \cdot \tilde{\epsilon} \cdot \vec{k})(\vec{k} \cdot \tilde{\mu} \cdot \vec{k}) - \epsilon_\perp \mu_\perp k_0^2 [\mu_\parallel (\vec{k} \cdot \tilde{\epsilon} \cdot \vec{k}) + \epsilon_\parallel (\vec{k} \cdot \tilde{\mu} \cdot \vec{k})] + k_0^4 \det(\tilde{\epsilon}) \det(\tilde{\mu}) = 0 \tag{8}$$

is obtained therefrom by imposing the condition $\det(\tilde{W}) = 0$. After the substitution of equations (1) and (2), the dispersion equation becomes factorable, thereby showing that the allowable wavevectors $\vec{k}$ are solutions of the following equations:

$$\vec{k} \cdot \tilde{\epsilon} \cdot \vec{k} = k_0^2 \mu_\perp \epsilon_\perp \epsilon_\parallel, \tag{9}$$

$$\vec{k} \cdot \tilde{\mu} \cdot \vec{k} = k_0^2 \mu_\perp \epsilon_\perp \mu_\parallel. \tag{10}$$

The plane waves that satisfy equation (9) constitute the so-called electric modes, whereas those that satisfy equation (10) are known as magnetic modes [26, 27].

Expressing the wavevector $\vec{k}_n^{(\ell)} = \alpha_n \hat{x} + \beta_n^{(\ell)} \hat{y}$ (either $\ell = E$ for modes of the electric type or $\ell = M$ for modes of the magnetic type) and then substituting $\vec{k} = \vec{k}_n^{(\ell)}$ into equation (9) or (10), we obtain quadratic equations for $\beta_n^{(\ell)}$ as functions of α_n, $|n| < \infty$ [29]. The vector $\vec{e}_n^{(\ell)}$ corresponding to each solution $\vec{k}_n^{(\ell)}$ is given via a non-zero column of the adjoint of $\tilde{W}$ [26, 28]. By virtue of the Faraday equation, we also define the vector

$$\vec{h}_n^{(\ell)} = \frac{1}{k_0} \tilde{\mu}^{-1} \cdot (\hat{k}_n^{(\ell)} \times \vec{e}_n^{(\ell)}), \quad \ell = E, M, \quad |n| < \infty. \tag{11}$$

With these definitions, we are able to write the following Floquet expansions that represent rigorously the electromagnetic fields in the region $y < \min g(x)$ [29]:

$$\vec{E}_2 = \sum_{n=-\infty}^{+\infty} \left[C_n^{(E)} \vec{e}_n^{(E)} \exp(\mathrm{i} \vec{k}_n^{(E)} \cdot \vec{r}) + C_n^{(M)} \vec{e}_n^{(M)} \exp(\mathrm{i} \vec{k}_n^{(M)} \cdot \vec{r}) \right], \tag{12}$$

$$\vec{H}_2 = \sum_{n=-\infty}^{+\infty} \left[C_n^{(E)} \vec{h}_n^{(E)} \exp(\mathrm{i} \vec{k}_n^{(E)} \cdot \vec{r}) + C_n^{(M)} \vec{h}_n^{(M)} \exp(\mathrm{i} \vec{k}_n^{(M)} \cdot \vec{r}) \right]. \tag{13}$$

Here, $\vec{k}_n^{(E)}$ and $\vec{k}_n^{(M)}$ denote those solutions of equations (9) and (10) which correspond to waves satisfying the radiation condition as $y \to -\infty$ [13]; whereas $C_n^{(E)}$ and $C_n^{(M)}$, $|n| \geqslant 0$, are unknown scalar coefficients quantifying the degree of diffraction into the uniaxial medium.

The tangential components of $\vec{E}_1$ and $\vec{E}_2$ must be equal at $y = g(x) \, \forall \, x$, and so must also be the tangential components of $\vec{H}_1$ and $\vec{H}_2$. These four boundary conditions must be satisfied by any method to find $\{R_n, S_n, C_n^{(E)}, C_n^{(M)}\}$, $|n| < \infty$.

2.2. Rayleigh method

For that purpose, we invoke the Rayleigh hypothesis [30]—that is, we assume that the expansions (3), (4), (12) and (13), which are strictly valid outside the corrugation region

max $g(x) > y >$ min $g(x)$, can be used to satisfy the usual conditions across the boundary $y = g(x)$. Generally speaking, the Rayleigh hypothesis gives valid results for smooth boundaries with corrugations that are not too deep. For sinusoidal gratings, this typically occurs when the corrugation depth does not exceed 0.3 times the period [31]. The limit of validity of methods based on the Rayleigh hypothesis has been investigated for impenetrable gratings [32, 33]; gratings made of isotropic penetrable materials [34], electrically uniaxial materials [35] or anisotropic absorbers [36]; and gyroelectromagnetic index-matched, periodically corrugated interfaces [37].

The family of functions $\exp(\mathrm{i}\,\alpha_m x)$, $|m| < \infty$, constitute the so-called Rayleigh basis. Introducing expansions (3), (4), (12) and (13) into the boundary conditions and thereafter projecting the resulting equations into the Rayleigh basis, we obtain a matrix equation for the diffraction amplitudes in terms of E_0 and H_0. In symbolic notation, this equation is written as

$$\begin{bmatrix} M_{11}^{-} & 0 & M_{13}^{-} & M_{14}^{-} \\ 0 & M_{22}^{-} & M_{23}^{-} & M_{24}^{-} \\ 0 & M_{32}^{-} & M_{33}^{-} & M_{34}^{-} \\ M_{41}^{-} & 0 & M_{43}^{-} & M_{44}^{-} \end{bmatrix} \begin{bmatrix} R_n \\ S_n \\ C_n^{(E)} \\ C_n^{(M)} \end{bmatrix} = \begin{bmatrix} M_{11}^{+}|_{m0} E_0 \\ M_{20}^{+}|_{m0} H_0 \\ M_{32}^{+}|_{m0} H_0 \\ M_{41}^{+}|_{m0} E_0 \end{bmatrix}, \tag{14}$$

where the elements of the block matrices are

$$\begin{aligned}
M_{11}^{\pm}|_{mn} &= \mp D_{mn}(\mp\beta_n^{(1)}), \\
M_{13}^{-}|_{mn} &= -(\vec{e}_n^{(E)} \cdot \hat{z}) D_{mn}(\beta_n^{(E)}), \\
M_{14}^{-}|_{mn} &= -(\vec{e}_n^{(M)} \cdot \hat{z}) D_{mn}(\beta_n^{(M)}), \\
M_{22}^{\pm}|_{mn} &= \frac{1}{k_0}[\pm \alpha_n E_{mn}(\mp\beta_n^{(1)}) + \beta_n^{(1)} D_{mn}(\mp\beta_n^{(1)})], \\
M_{23}^{-}|_{mn} &= -(\vec{e}_n^{(E)} \cdot \hat{y}) E_{mn}(\beta_n^{(E)}) - (\vec{e}_n^{(E)} \cdot \hat{x}) D_{mn}(\beta_n^{(E)}), \\
M_{24}^{-}|_{mn} &= -(\vec{e}_n^{(M)} \cdot \hat{y}) E_{mn}(\beta_n^{(M)}) - (\vec{e}_n^{(M)} \cdot \hat{x}) D_{mn}(\beta_n^{(M)}), \\
M_{32}^{\pm}|_{mn} &= M_{11}^{\pm}|_{mn}, \\
M_{33}^{-}|_{mn} &= -(\vec{h}_n^{(E)} \cdot \hat{z}) D_{mn}(\beta_n^{(E)}), \\
M_{34}^{-}|_{mn} &= -(\vec{h}_n^{(M)} \cdot \hat{z}) D_{mn}(\beta_n^{(M)}), \\
M_{41}^{\pm}|_{mn} &= \frac{1}{k_0}[\mp \alpha_n E_{mn}(\mp\beta_n^{(1)}) - \beta_n^{(1)} D_{mn}(\mp\beta_n^{(1)})], \\
M_{43}^{-}|_{mn} &= -(\vec{h}_n^{(E)} \cdot \hat{y}) E_{mn}(\beta_n^{(E)}) - (\vec{h}_n^{(E)} \cdot \hat{x}) D_{mn}(\beta_n^{(E)}), \\
M_{44}^{-}|_{mn} &= -(\vec{h}_n^{(M)} \cdot \hat{y}) E_{mn}(\beta_n^{(M)}) - (\vec{h}_n^{(M)} \cdot \hat{x}) D_{mn}(\beta_n^{(M)}),
\end{aligned} \tag{15}$$

with

$$D_{mn}(u) = \int_0^d \exp\left[\mathrm{i}\frac{2\pi}{d}(n-m)x + \mathrm{i}\,u g(x)\right] \mathrm{d}x, \tag{16}$$

$$E_{mn}(u) = \int_0^d g'(x) \exp\left[\mathrm{i}\frac{2\pi}{d}(n-m)x + \mathrm{i}\,u g(x)\right] \mathrm{d}x. \tag{17}$$

(The prime denotes differentiation with respect to the argument.)

On restricting the sums in equations (3), (4), (12) and (13) to $|n| \leqslant N$, the infinite system (14) becomes a system of $8N + 4$ linear equations with $8N + 4$ unknowns: R_n, S_n, $C_n^{(E)}$ and $C_n^{(M)}$, $n \in (-N, N)$. For all calculated results presented in the following section, the value of N was selected to satisfy the principle of conservation of energy within a tolerance of $\pm 10^{-6}$.

After the determination of the Floquet expansion coefficients, the diffraction efficiencies for the propagating planewave components of the reflected or refracted fields can be calculated as the ratio between the diffracted and the incident intensities. These diffraction efficiencies are defined as

$$\rho_n = \frac{\mathrm{Re}[\beta_n^{(1)}]}{\beta_0^{(1)}} \frac{|R_n|^2 + |S_n|^2}{|E_0|^2 + |H_0|^2}, \tag{18}$$

for the reflected Floquet harmonics, and

$$\tau_n^{(\ell)} = -\frac{|C_n^{(\ell)}|^2}{|E_0|^2 + |H_0|^2} \frac{\mathrm{Re}[\beta_n^{(\ell)}]}{\beta_n^{(\ell)}} \frac{k_0}{\beta_0^{(1)}} \mathrm{Re}\{[\vec{e}_n^{(\ell)} \times (\vec{h}_n^{(\ell)})^*] \cdot \hat{y}\}, \quad \ell = E, M, \tag{19}$$

for the refracted Floquet harmonics, with the asterisk denoting the complex conjugate and Re denoting the 'real part'.

3. Numerical results and discussion

3.1. Classification of constitutive tensors

Our focus being on gratings of anisotropic NPV materials, it is best to delineate certain relevant properties of the relative permittivity and the relative permeability tensors. In order to unambiguously distinguish between propagating and evanescent Floquet harmonics in the diffracting medium, we set both tensors to be Hermitian. As the tensors (1) and (2) are real symmetric, each can be classified as (i) positive definite, (ii) negative definite or (iii) indefinite [38]. If all eigenvalues of a real symmetric tensor are >0, it is positive definite; if all eigenvalues are <0, it is negative definite; but if it has both negative and positive eigenvalues, then it is indefinite. In the present context, we exclude constitutive tensors with null eigenvalues.

Thus, the relative permittivity tensor (1) is positive definite if $\epsilon_\perp > 0$ and $\epsilon_\parallel > 0$; it is negative definite if $\epsilon_\perp < 0$ and $\epsilon_\parallel < 0$; and it is indefinite if $\epsilon_\perp \epsilon_\parallel < 0$. A similar classification applies to the relative permeability tensor (2). If both $\tilde{\epsilon}$ and $\tilde{\mu}$ are positive definite, the material is of the PPV kind.

3.2. Cases chosen for investigation

The diffracting medium is transversely isotropic, i.e. it is isotropic in the plane to which its optic axis is normal. The plane of incidence being the xy plane, the anisotropy of the diffracting medium would be essentially inconsequential if $\hat{c} = \hat{z}$. In order to eliminate the effects of transverse isotropy, we chose $c_z = 0$ for numerical investigation. As distinct from the boundary-value problem for isotropic NPV gratings [21]–[23], the problem stated in section 2.1 is not always separable for two independent polarization states or modes and generally involves a full vectorial approach, as can be gleaned from equation (14). For the sake of simplicity

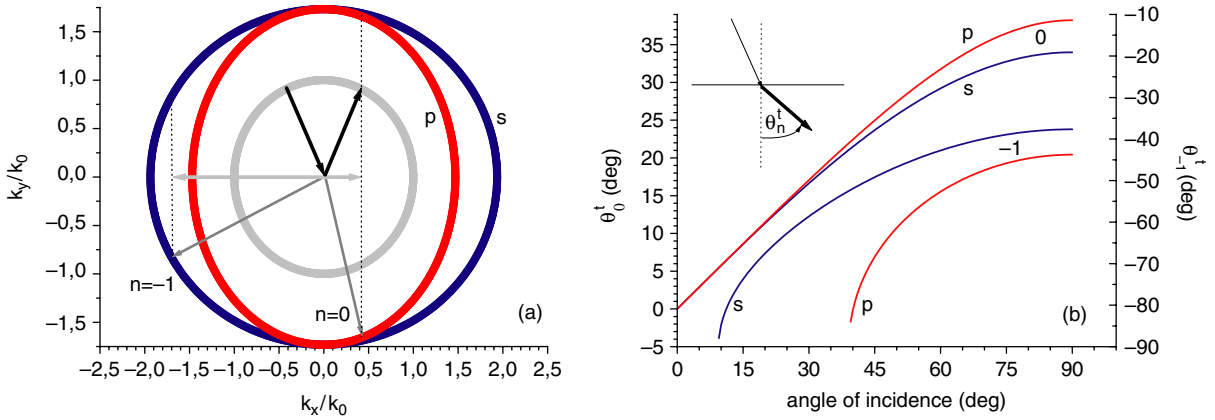

Figure 1. (a) Reciprocal space map for $\epsilon_\perp = 2.5$, $\epsilon_\parallel = 1.8$, $\mu_\perp = 1.2$, $\mu_\parallel = 1.5$ and $\hat{c} = \hat{y}$; $k_x = \vec{k} \cdot \vec{x}$ and $k_y = \vec{y} \cdot \vec{x}$. The value $k_0 d = 2\pi/2.1$ is indicated by the horizontal, light-grey double-arrow. (b) Relationship of the angle of incidence θ_0 and the angle θ_n^t between the wavevector of the refracted Floquet harmonic of order n and the $-y$ axis, when $k_0 d = 2\pi/2.1$. Magnetic type (s-polarized): blue curves; electric type (p-polarized): red curves.

and without sacrificing the distinctive features of anisotropy, we confine ourselves here to situations wherein the diffracted fields have the same linear polarization state as the incident plane wave. Specifically, we assume that

- the optic axis is either perpendicular ($\hat{c} = \hat{y}$) or parallel ($\hat{c} = \hat{x}$) to the mean corrugation plane ($y = 0$), and lies in the plane of incidence; and
- the incident plane wave is either s-polarized ($H_0 = 0$) or p-polarized ($E_0 = 0$).

Let us note that the separation of linear polarization states is not generally possible when $\hat{c} = \hat{x}\cos\gamma + \hat{z}\sin\gamma$, unless $\gamma = q\pi/2$, $q = 0, 1, 2, \ldots$.

For the constitutive tensors of the diffracting medium, we consider two cases as well:

- Case I: either both $\tilde{\epsilon}$ and $\tilde{\mu}$ are positive definite, or both are negative definite. These two are referred to as cases IP and IN in the remainder of this paper. Case IP provides a PPV reference to compare and evaluate the results for NPV gratings.
- Case II: both $\tilde{\epsilon}$ and $\tilde{\mu}$ are indefinite.

As can be deduced from equations (9) and (10), the reciprocal space map $(\vec{k} \cdot \vec{x},\ \vec{k} \cdot \vec{y})$ for plane waves propagating in the diffracting medium and for these orientations of the optic axis is elliptic for case I, but hyperbolic for case II.

3.3. Case I

Let us begin with case IP with $\hat{c} = \hat{y}$ and the incident plane wave being either s- or p-polarized. The reciprocal space map for plane waves propagating in the xy plane is shown in figure 1(a) for $\epsilon_\perp = 2.5$, $\epsilon_\parallel = 1.8$, $\mu_\perp = 1.2$ and $\mu_\parallel = 1.5$.

The inner circle

$$\alpha_n^2 + (\beta_n^{(1)})^2 = k_0^2 \tag{20}$$

(light grey in figure 1(a)) corresponds to plane waves in the medium of incidence, whereas the outer ellipse

$$\frac{\alpha_n^2}{\mu_\parallel} + \frac{(\beta_n^{(M)})^2}{\mu_\perp} = k_0^2 \epsilon_\perp \tag{21}$$

(blue curve in figure 1(a)) describes waves of the magnetic type (s-polarized for $\hat{c} = \hat{y}$) and the inner ellipse

$$\frac{\alpha_n^2}{\epsilon_\parallel} + \frac{(\beta_n^{(E)})^2}{\epsilon_\perp} = k_0^2 \mu_\perp \tag{22}$$

(red curve in figure 1(a)) describes waves of the electric type (p-polarized for $\hat{c} = \hat{y}$) in the diffracting medium. From this map and from equations (5) for α_n and $\beta_n^{(1)}$, we conclude that if the frequency is chosen so that $k_0 d = 2\pi/2.1$ (as indicated by the horizontal, light-grey double-arrow in figure 1(a)), $\beta_n^{(1)}$ is real-valued only for $n = 0$. Then the grating acts like a flat interface, in the sense that only the specularly reflected Floquet harmonic can propagate in the medium of incidence for any angle of incidence.

Besides, as the semiaxes (along the x axis) of the ellipses described by equations (21) and (22) for the chosen constitutive scalars are $(\epsilon_\perp \mu_\parallel)^{1/2} = 1.93$ and $(\mu_\perp \epsilon_\parallel)^{1/2} = 1.47$ respectively, only the two specularly refracted harmonics (of the electric and magnetic types with $n = 0$), but no non-specularly refracted harmonics, can exist in the diffracting medium for near-normal incidence. Taking into account that

- the energy–velocity direction is normal to the dispersion curve, and
- the sign of the projection of the energy–velocity direction along the phase-velocity direction is given by the sign of $\epsilon_\perp$ for magnetic waves and by the sign of $\mu_\perp$ for electric waves [16], for propagation in the plane containing the optic axis,

we conclude that the phase and energy velocities of both refracted waves are nearly (exactly) parallel for near-normal (normal) incidence. So, the grating acts as a positively refracting interface, in the sense that both refracted rays (i.e., the energy fluxes) bend towards the normal to the mean corrugation plane and never emerge on the same side of the normal as the incident ray [15].

Changing the signs of all four constitutive scalars to go from case IP to case IN does not affect the shape of the reciprocal space map, as may be concluded by comparing figures 1(a) and 2(a). Therefore, for $k_0 d = 2\pi/2.1$, the grating still acts like a flat interface supporting only refracted Floquet harmonics of the electric and magnetic types and of order $n = 0$ under near-normal incidence conditions. However, as the directions of the phase and the energy velocities of both of the refracted harmonics are now nearly (exactly) antiparallel for near-normal (normal) incidence, both the refracted rays emerge on the same side of the normal to the mean corrugation plane as the incident ray; therefore, the grating acts as a negatively refracting interface.

The graphical construction to find the wavevectors for the specularly refracted wave ($n = 0$) of the electric type is indicated in figure 1(a) for case IP and in figure 2(a) for case IN, when

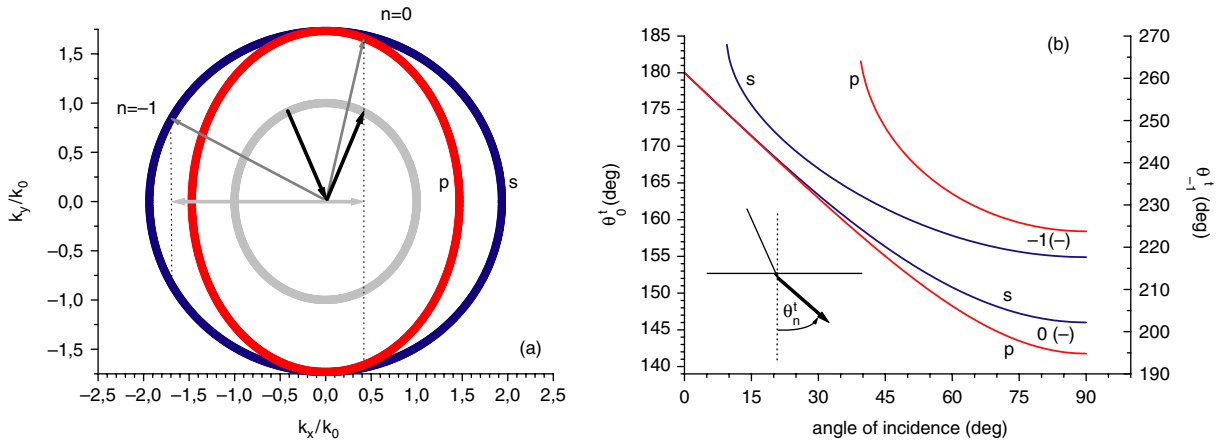

Figure 2. Same as figure 1, but for $\epsilon_\perp = -2.5$, $\epsilon_\parallel = -1.8$, $\mu_\perp = -1.2$ and $\mu_\parallel = -1.5$.

the angle of incidence $\theta_0 \approx 24^\circ$.[5] Unlike the near-normal incidence situation, a non-specularly refracted Floquet harmonic ($n = -1$) of the magnetic type can also propagate for this angle of incidence. The construction of the wavevector is shown in figure 1(a), where the horizontal double arrow indicates the quantity $2\pi/d = 2.1/k_0$: both the wavevector and ray emerge on the same side of the normal as the incident ray for case IP, whereas the wavevector corresponds to an energy flux bent towards the interface normal with respect to the incident ray for case IN. The relationship of the angle of refraction to the angle of incidence is shown in figures 1(b) and 2(b).

In the absence of corrugations (i.e. $g(x) = 0$), the diffraction efficiencies (i.e. the specular reflectances and transmittances) due to the boundary between vacuum and either an NPV material or its PPV analogue are identical [20, 39]. But differences should be evident when the boundary is corrugated, even when all non-specularly refracted harmonics are evanescent for the chosen value of $k_0 d$. Such an expectation, supported by known results for isotropic NPV and PPV gratings [21]–[23], is indeed borne out for the anisotropic gratings—as evinced by the diffraction efficiency plots in figure 3 for the sinusoidal corrugation $g(x) = 0.5h \cos(2\pi x/d)$ with $h/d = 0.1$ and the same constitutive properties and incidence conditions as for figures 1 and 2. As θ_0 increases from 0, the diffraction efficiencies show evidence of weak Rayleigh–Wood anomalies [40]

- at $\theta_0 \approx 9.41^\circ$, a value at which the refracted Floquet harmonic of the magnetic type and order $n = -1$ changes from being evanescent to propagating, and
- at $\theta_0 \approx 39.07^\circ$, a value at which the refracted Floquet harmonic of the electric type and order $n = -1$ changes similarly.

The diffraction efficiencies of these non-specular refracted harmonics (figure 3(c)) are more sensitive than of their specular counterparts (figure 3(b)) to the type of the diffracting medium. Indeed, a comparison of figures 3(c) and 4(c), for $h/d = 0.1$ and 0.3 respectively, supports that conclusion.

[5] Wavevectors for refracted waves of the magnetic type with $n = 0$ have nearly the same direction, and are therefore not shown for the sake of clarity.

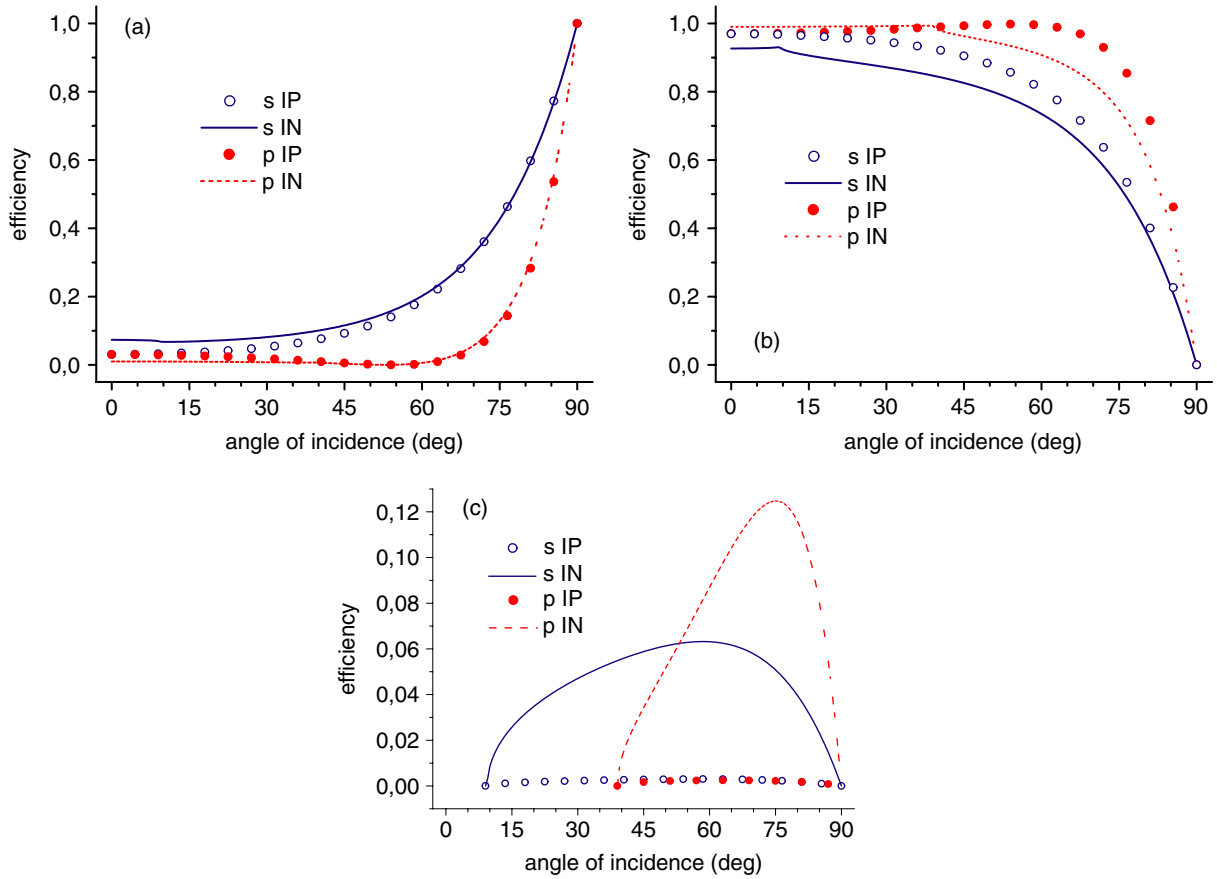

Figure 3. Diffraction efficiencies for a sinusoidal corrugation $g(x) = 0.5h \cos(2\pi x/d)$ with $h/d = 0.1$. The incident wave is either s- or p-polarized and the diffracting medium has either all positive constitutive scalars (case IP) or all negative constitutive scalars (case IN); $\epsilon_\perp = \pm 2.5$, $\epsilon_\parallel = \pm 1.8$, $\mu_\perp = \pm 1.2$, $\mu_\parallel = \pm 1.5$ and $\vec{c} = \vec{y}$, For s-polarized (p-polarized) incidence, the refracted waves are only of the magnetic (electric) type. (a) Specular reflection ($n = 0$), (b) specular refraction ($n = 0$) and (c) non-specular refraction of order $n = -1$.

There is no need to present results for $\hat{c} = \hat{x}$ for cases IP and IN, as our conclusions were qualitatively similar to that for $\hat{c} = \hat{y}$. In fact, we made similar conclusions for all other orientations of the optic axis in the xy plane.

3.4. Case II

Either all four constitutive scalars of the diffracting medium are positive or all four are negative in section 3.3. In contrast, we now examine the cases when $\epsilon_\parallel \epsilon_\perp < 0$ and $\mu_\parallel \mu_\perp < 0$. As for case I, when the incident plane wave is either s- or p-polarized, the polarization state is not changed upon reflection and refraction, provided that the optic axis lies in the xy plane.

Furthermore, for numerical illustration, we maintained the value of $k_0 d = 2\pi/2.1$, so that only the specularly reflected Floquet harmonic can propagate in the medium of incidence for

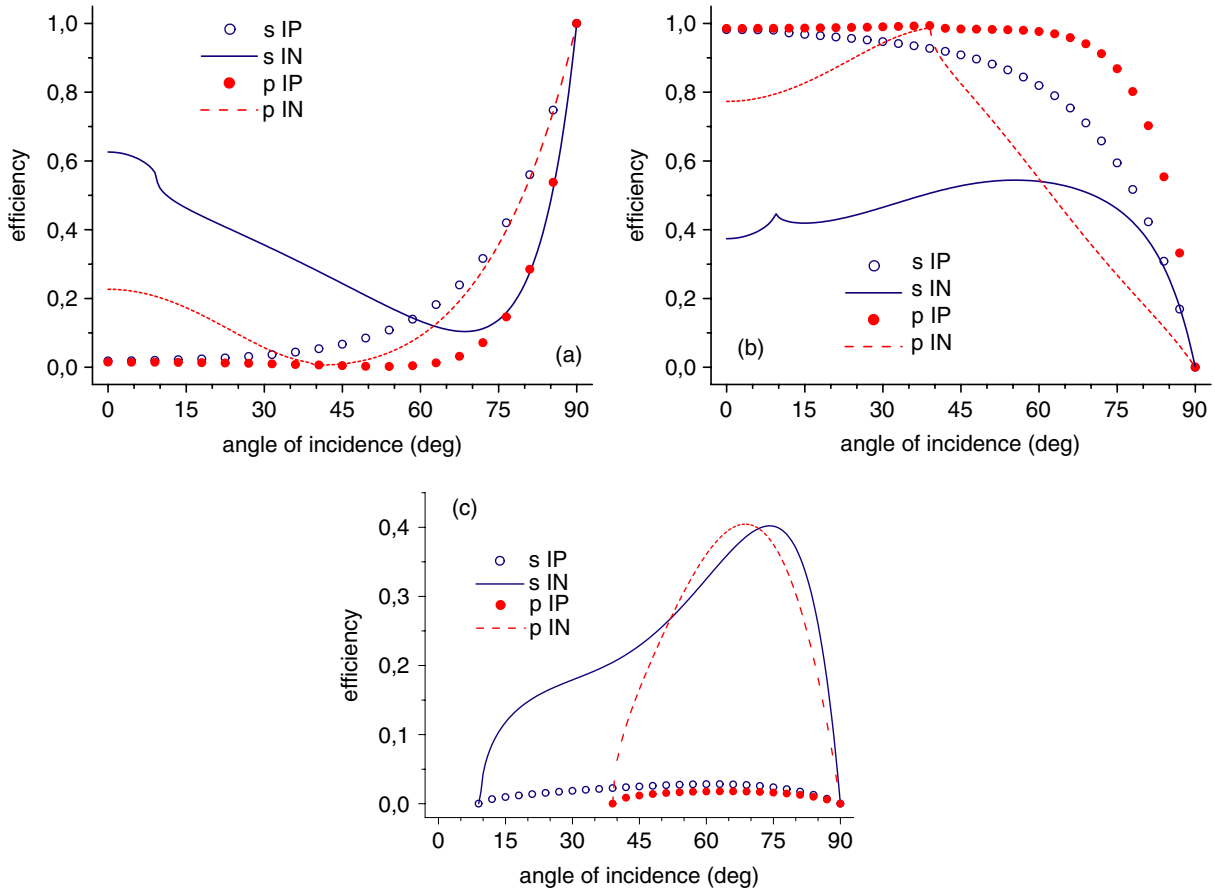

Figure 4. Same as figure 3, except that $h/d = 0.3$.

any angle of incidence. For illustration of diffractive effects, we chose

- Case IIA: $\epsilon_\perp = -2.5$, $\epsilon_\parallel = 1.8$, $\mu_\perp = 1.2$, $\mu_\parallel = -1.5$ and $\hat{c} = \hat{x}$;
- Case IIB: $\epsilon_\perp = +2.5$, $\epsilon_\parallel = -1.8$, $\mu_\perp = -1.2$, $\mu_\parallel = +1.5$ and $\hat{c} = \hat{x}$;
- Case IIC: $\epsilon_\perp = -2.5$, $\epsilon_\parallel = 1.8$, $\mu_\perp = 1.2$, $\mu_\parallel = -1.5$ and $\hat{c} = \hat{y}$; and
- Case IID: $\epsilon_\perp = +2.5$, $\epsilon_\parallel = -1.8$, $\mu_\perp = -1.2$, $\mu_\parallel = +1.5$ and $\hat{c} = \hat{y}$.

The conclusions gleaned from studying these four cases hold not merely for the chosen sets of the constitutive scalars but all other sets satisfying the conditions delineated for case II. Furthermore, in order to concentrate on the refracting properties of the anisotropic medium with hyperbolic dispersion curves, we excluded cases for which $\epsilon_\parallel \mu_\perp < 0$ and $\epsilon_\perp \mu_\parallel < 0$, where only one type of refracted harmonics, either electric or magnetic, are evanescent for all angles of incidence.

3.4.1. Cases IIA and IIB. Let us begin with cases IIA and IIB. The dispersion equation for the diffracting medium is

$$\frac{\alpha_n^2}{\mu_\perp} + \frac{(\beta_n^{(M)})^2}{\mu_\parallel} = k_0^2 \epsilon_\perp \tag{23}$$

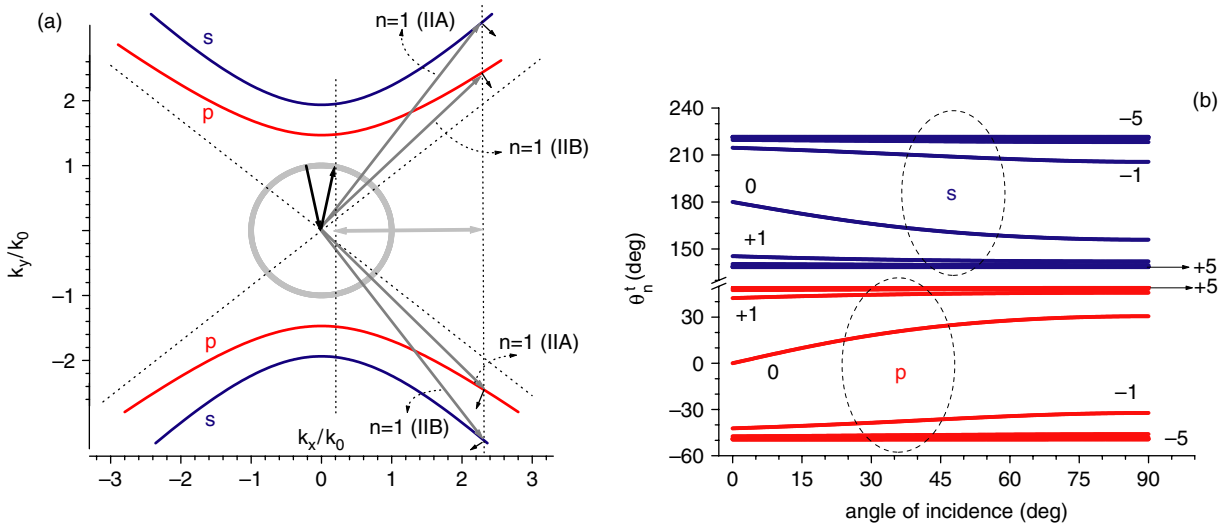

Figure 5. (a) Reciprocal space map for $\epsilon_\perp = \mp 2.5$, $\epsilon_\parallel = \pm 1.8$, $\mu_\perp = \pm 1.2$, $\mu_\parallel = \mp 1.5$ and $\hat{c} = \hat{x}$; $k_x = \vec{k} \cdot \hat{x}$ and $k_y = \vec{k} \cdot \hat{y}$. The value $k_0 d = 2\pi/2.1$ is indicated by the horizontal, light-grey double-arrow. The little arrows perpendicular to the hyperbolas indicate the direction of energy transport associated with each wavevector. Dotted lines indicate the asymptotes of the hyperbola associated with electric modes in the diffracting medium. (b) Relationship of the angle of incidence θ_0 and the angle θ_n^t between the wavevector of the refracted Floquet harmonic of order n and the $-y$ axis for case IIA, when $k_0 d = 2\pi/2.1$. Replace θ_n^t by $-\theta_n^t$ for case IIB. Magnetic type (s-polarized): blue curves; electric type (p-polarized): red curves.

for Floquet harmonics of the magnetic type (s-polarized for $\hat{c} = \hat{x}$), and

$$\frac{\alpha_n^2}{\epsilon_\perp} + \frac{(\beta_n^{(E)})^2}{\epsilon_\parallel} = k_0^2 \mu_\perp \tag{24}$$

for Floquet harmonics of the electric type (p-polarized for $\hat{c} = \hat{y}$). These equations are similar to equations (21) and (22), respectively. But there is a major difference due to the signs of the constitutive scalars in cases IIA and IIB: these dispersion equations now describe hyperbolas, not ellipses.

The reciprocal space maps for both cases IIA and IIB are shown in figure 5(a). The outer hyperbolas correspond to refracted harmonics of the magnetic type and the inner hyperbolas correspond to refracted harmonics of the electric type in the diffracting medium; whereas the circle refers to harmonics in the medium of incidence. Repeating in figure 5(a) the graphical constructions described for figures 1(a) and 2(a), we conclude that the dispersion equation for the Floquet harmonic of order n in the diffracting medium has real-valued solutions for all n. This is in huge contrast not only to case I but also to all gratings made of conventional materials, for which the dispersion equation for the Floquet harmonics has real-valued solutions only in a limited n-range [40]–[43].

Therefore we can state that gratings made of uniaxial materials with indefinite $\tilde{\epsilon}$ and $\tilde{\mu}$ can refract an incident plane wave into propagating Floquet harmonics exclusively. In contrast,

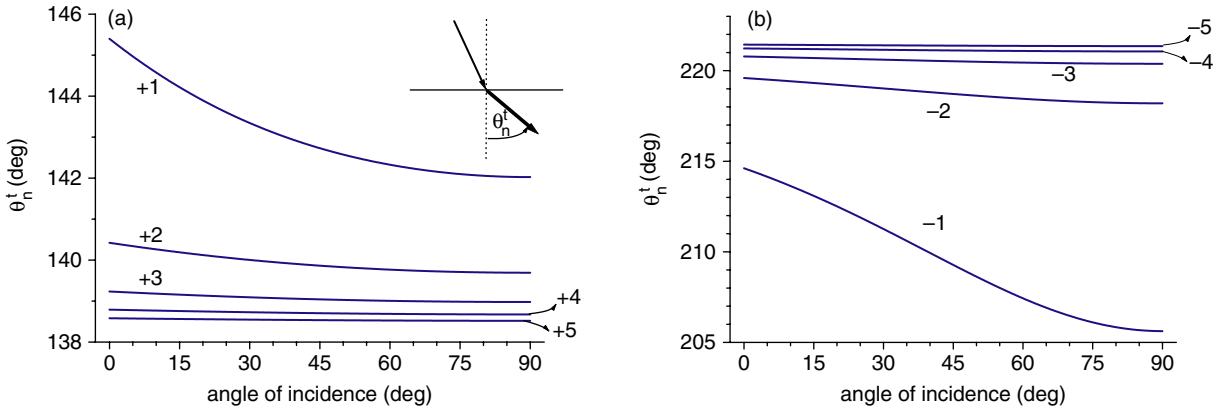

Figure 6. Relationship of the angle of incidence θ_0 and the angle θ_n^t between the wavevector of the refracted Floquet harmonic of order n and the $-y$ axis for case IIA, when $k_0 d = 2\pi/2.1$ and the refracted harmonics are of the magnetic type. (a) $n > 0$ and (b) $n < 0$.

refraction by conventional gratings consists of a few propagating and the remaining evanescent Floquet harmonics. The infinite set of propagating Floquet harmonics for cases IIA and IIB can be readily deduced from the graphical construction in figure 5(a) by noting that there is always a theoretically possible direction of energy flux associated with these harmonics, lying along the normal to the dispersion curves and pointing towards $y < 0$ as required by the radiation condition.

Referring to the construction shown in figure 5(a), we observe that the refracted wavevectors corresponding to $n = 1$ lie inside the angular region delimited by the asymptotes of the inner hyperbola (dotted lines) and containing the $k_y = \bar{k} \cdot \hat{y}$ axis. A similar construction for other values of n shows that all the refracted wavevectors are always inside the same region, delimited by the asymptotes of the inner hyperbola (which corresponds to modes of the electric type, for both cases IIA and IIB in figure 5(a)). The relationship of θ_n^t-to-θ_0 is shown in figure 5(b), which demonstrates that the refracted wavevectors for high $|n|$ are concentrated in narrow angular sectors delineated by the asymptotes of the hyperbolas in figure 5(a). For $k_0 d = 2\pi/2.1$, the only refracted orders with substantial variation in direction with the angle of incidence are the ones with $|n| < 2$. To further appreciate the characteristic angular separation between the refracted orders, in figure 6 we present the θ_n^t-to-θ_0 relationships for Floquet harmonics of positive (figure 6(a)) and negative (figure 6(b)) orders and of the magnetic type.

The direction of the energy flux associated with the refracted waves (i.e. the direction of the refracted rays) is along the normal to the dispersion curves and pointing towards the $-y$ axis (as required by the radiation condition). For $\hat{c} = \hat{x}$, let the angle between the ray direction of the refracted Floquet harmonic of order n and the $-y$ axis be denoted by ξ_n^t. Then,

$$\sin \xi_n^t = \frac{\sin \theta_n^t}{\mu_\perp}, \qquad \cos \xi_n^t = \frac{\cos \theta_n^t}{\mu_\parallel} \tag{25}$$

for harmonics of the magnetic type, and

$$\sin \xi_n^t = \frac{\sin \theta_n^t}{\epsilon_\perp}, \qquad \cos \xi_n^t = \frac{\cos \theta_n^t}{\epsilon_\parallel} \tag{26}$$

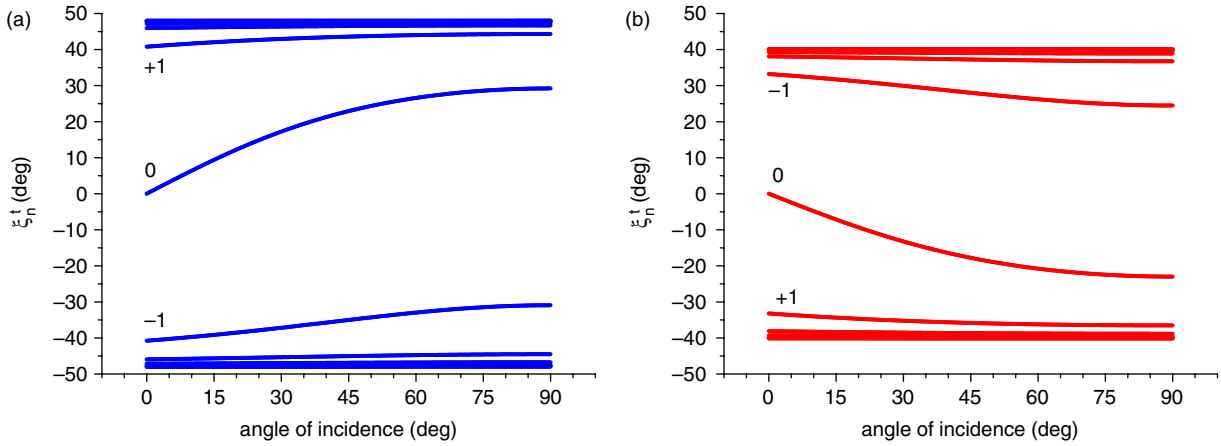

Figure 7. Relationship of the angle of incidence θ_0 and the angle ξ_n^t between the ray direction of the refracted Floquet harmonic of order n and the $-y$ axis for case IIA, when $k_0 d = 2\pi/2.1$. (a) Magnetic type and (b) electric type.

for harmonics of the electric type. Thus, for refracted harmonics of the electric type, the wavevector and the ray direction are oriented either on the same side or on opposite sides of the y axis, depending on $\epsilon_\parallel$ being positive or negative, respectively, whereas for refracted harmonics of the magnetic type, it is the sign of $\mu_\parallel$ which determines if the two vectors are oriented on the same side or on opposite sides of the y axis. Accordingly, for case IIA, the refracted Floquet harmonics are counterposed [15] only when the incident plane wave is s-polarized, whereas counterposition occurs only for the p-polarized incidence for case IIB.

The relationship of the the ray angles ξ_n^t with θ_0 is shown in figure 7 for refracted Floquet harmonics of the magnetic (figure 7(a)) and electric (figure 7(b)) types, for case IIA. We note that although the wavevector and the ray direction are counterposed for magnetic types, the specularly refracted ray ($n = 0$) never emerges on the same side of the y axis as the incident ray; i.e. $\xi_0^t > 0$, just as for positively refracting interfaces. The same happens for refracted Floquet harmonics of order $n > 0$. In contrast, the wavevector and the ray direction are not counterposed for refracted harmonics of the electric type—$\xi_0^t < 0$ as for negatively refracting interfaces.

In the absence of corrugations, the diffraction efficiencies are identical for cases IIA and IIB. But an infinite number of refraction channels are available when the interface is corrugated even weakly. The kinematic arguments used up to this point, based on the analysis of reciprocal space maps, only show that energy can be transported by the infinite set of refracted Floquet harmonics, but do not give further information about the diffraction efficiencies. For that purpose, a boundary-value problem must be solved.

All theoretical methods available for gratings made of conventional materials rely on restricting the Floquet harmonics to $|n| \leqslant N$, and the adequacy of the results is studied by checking convergence against N and the fulfilment of physical tests (such as on the conservation of energy and reciprocity) [40, 41]. An adequate value of N for conventional gratings is such that all propagating and some evanescent Floquet harmonics on both sides of the corrugated boundary are covered. But no evanescent harmonics can exist in the diffracting medium for cases IIA and IIB, which means that particular care must be taken to choose N.

With the Rayleigh method described in section 2.2, we found good convergence with $N \leqslant 7$ for both cases IIA and IIB for a sinusoidal corrugation $g(x) = 0.5h \cos(2\pi x/d)$ with $h/d = 0.1$.

Table 1. Reflection (ρ) and some refraction (τ) efficiencies for a sinusoidal grating $g(x) = 0.05d\cos(2\pi x/d)$ for cases IIA and IIB, when the incident plane wave is either s- or p-polarized; $\theta_0 = 15^\circ$, $k_0 d = 2\pi/2.1$ and $N = 7$.

Efficiency	s (IIA)	p (IIA)	s (IIB)	p (IIB)
ρ_0	0.1540×10^{-1}	0.5880×10^{-2}	0.2098×10^{-1}	0.8506×10^{-2}
τ_{-3}	0.1952×10^{-3}	0.2423×10^{-5}	0.7361×10^{-6}	0.6619×10^{-4}
τ_{-2}	0.2260×10^{-2}	0.5039×10^{-4}	0.1217×10^{-4}	0.1236×10^{-2}
τ_{-1}	0.4548×10^{-1}	0.2638×10^{-2}	0.2020×10^{-2}	0.3700×10^{-1}
τ_0	0.8813	0.9872	0.9685	0.9149
τ_1	0.5170×10^{-1}	0.4155×10^{-2}	0.8165×10^{-2}	0.3669×10^{-1}
τ_2	0.3314×10^{-2}	0.8779×10^{-4}	0.3147×10^{-3}	0.1521×10^{-2}
τ_3	0.3182×10^{-3}	0.4046×10^{-5}	0.2558×10^{-4}	0.9005×10^{-4}

The results presented in table 1, where we have provided the diffraction efficiencies for $\theta_0 = 15^\circ$, show that little power is coupled into the higher-order refracted harmonics for the chosen grating geometry, thus ensuring convergence and the satisfaction of the principle of conservation of energy with 15 Floquet harmonics. Figure 8 shows plots of the diffraction efficiencies against θ_0, indicating that the reversal of signs of all four constitutive scalars leads to effects that are exactly the same as for case I (figure 3).

When we increased the corrugation depth to $h/d = 0.2$, we were unable to obtain convergent results. The fact that the Rayleigh method works well for gratings of conventional anisotropic materials for $h/d \leqslant 0.3$ [35] (as in our previous example in figure 4) suggests that the lack of convergence observed here

- is related to the existence of an infinite number of propagating refracted harmonics, and
- should be common to all known theoretical methods for gratings, when applied to diffraction materials with hyperbolic dispersion equations.

These issues are currently under investigation, and we shall present our results elsewhere in due course.

3.4.2. Cases IIC and IID. Cases IIC and IID are similar to cases IIA and IIB, respectively, except that the optic axis is perpendicular to the mean corrugation plane ($\hat{c} = \hat{y}$). The dispersion equations in the diffracting medium are still the same as equations (21) and (22), but the dispersion curves are hyperbolas instead of ellipses.

The reciprocal space map for cases IIC and IID is exemplified in figure 9(a). The outer hyperbolas correspond to refracted harmonics of the magnetic type (s-polarized for $\hat{c} = \hat{y}$), the inner hyperbolas correspond to refracted harmonics of the electric type (p-polarized for $\hat{c} = \hat{y}$) and the circle to harmonics in the medium of incidence. The graphical construction shown in figure 9(a) shows that when the corrugations are absent ($g(x) \equiv 0$), incident plane waves are totally reflected for all angles of incidence and both linear polarization states, because the dispersion equations for the diffracting medium do not have real-valued solutions. This is a particular case of the anomalous total reflection phenomenon reported by Hu and Chui [16], so labelled because it occurs when the angle of incidence is smaller, but not larger, than a critical angle—in contrast with the usual total reflection phenomenon that occurs only if the angle of

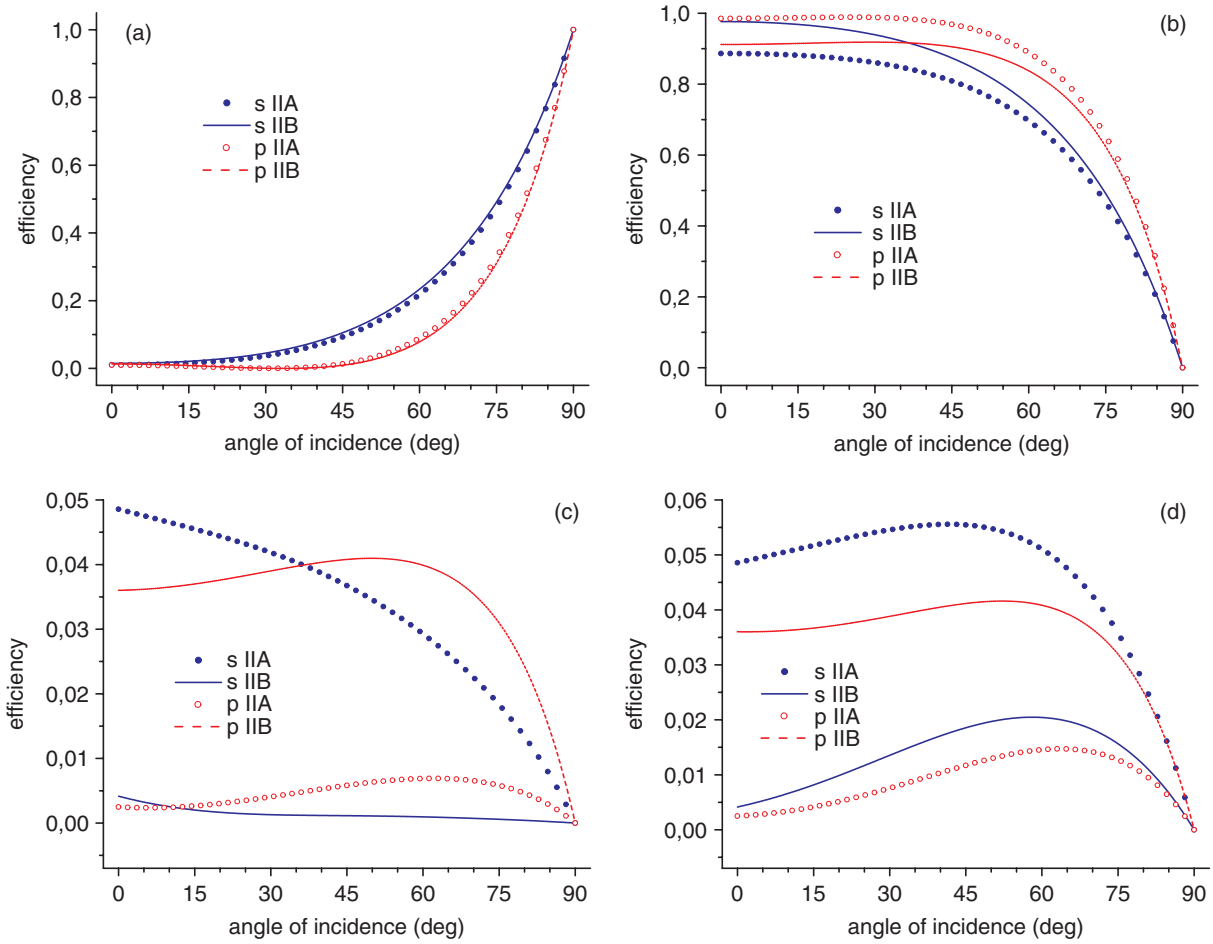

Figure 8. Diffraction efficiencies for a sinusoidal corrugation $g(x) = 0.5h\cos(2\pi x/d)$ with $h/d = 0.1$. The incident plane wave is either s- or p-polarized and the diffracting medium is described either by case IIA or IIB. (a) Specular reflection ($n = 0$), (b) specular refraction ($n = 0$), (c) non-specular refraction of order $n = -1$ and (d) non-specular refraction of order $n = -2$.

incidence is larger, but not smaller, than a critical angle [42]. We note that for the constitutive scalars chosen for section 3.4.2, the anomalous total reflection angle is $\pi/2$; thus, in the absence of corrugations, the boundary acts as an omnidirectional totally reflecting interface.

Repeating in figure 9(a) the graphical constructions described for figures 1(a) and 2(a), we deduce the two following conclusions for cases IIC and IID.

- Firstly, specularly refracted harmonics are never allowed to propagate in this kind of grating. This is a direct consequence for periodically corrugated surfaces of the anomalous total reflection phenomenon for flat interfaces. Of course, the present-day construction of NPV metamaterials is such that the boundary is periodically stepped [24], which would subvert the anomalous total refraction phenomenon.
- Secondly, as for cases IIA and IIB, the relevant dispersion equation for the Floquet harmonics in the diffracting material has an infinite number of real-valued solutions—but only for $|n| \geqslant n_{\min} > 0$. As an example, for the incidence condition depicted in figure 9(a), the

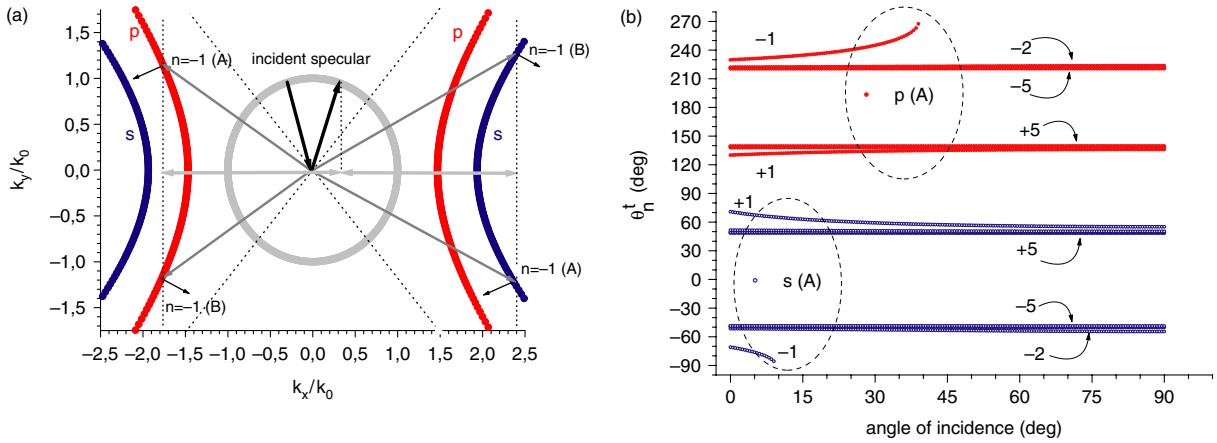

Figure 9. Reciprocal space map for $\epsilon_\perp = \mp 2.5$, $\epsilon_\parallel = \pm 1.8$, $\mu_\perp = \pm 1.2$, $\mu_\parallel = \mp 1.5$ and $\hat{c} = \hat{y}$; $k_x = \vec{k} \cdot \vec{x}$ and $k_y = \vec{y} \cdot \vec{x}$. (b) Relationship of the angle of incidence θ_0 and the angle θ_n^t between the wavevector of the refracted Floquet harmonic of order n and the $-y$ axis for case IIC, when $k_0 d = 2\pi/2.1$. Replace θ_n^t by $-\theta_n^t$ for case IID. Magnetic type (s-polarized): blue curves; electric type (p-polarized): red curves.

specularly refracted Floquet harmonics of both types as well as the non-specularly refracted Floquet harmonic of order $n = -1$ and the magnetic type are the only non-propagating harmonics; whereas all other Floquet harmonics ($n \neq -1$ and $n \neq 0$), whether of the electric or the magnetic type, are non-evanescent. On increasing the angle of incidence, the refracted Floquet harmonic of order $n = -1$ of the electric type ceases to propagate when $\sin\,\theta_0$ exceeds $2\pi/k_0 d - \mu_\perp \epsilon_\parallel$, the transition value being $\theta_0 \approx 30.07^\circ$ for the chosen constitutive scalars.

Thus, again we encounter a class of gratings which can refract into an infinite number of channels. In figure 9(a), we observe that the refracted wavevectors corresponding to $n = \pm 1$ lie inside the angular region delimited by the asymptotes of the inner hyperbola (dotted lines) and containing the $k_x = \vec{k} \cdot \hat{x}$ axis. A similar argument for other values of n shows that all the refracted wavevectors are always inside the same region, delimited by the asymptotes of the inner hyperbola (which corresponds to modes of the electric type, for both cases IIC and IID in figure 9(a)). The relationship of θ_n^t to θ_0 is shown in figure 9(b), which demonstrates that the refracted wavevectors for high $|n|$ are concentrated in narrow angular sectors defined by the asymptotes of the hyperbolas in figure 9(a).

For $\hat{c} = \hat{y}$, the angle ξ_n^t between the ray direction of the refracted Floquet harmonic of order n and the $-y$ axis is delineated by

$$\sin\,\xi_n^t = \frac{\sin\,\theta_n^t}{\mu_\parallel}, \qquad \cos\,\xi_n^t = \frac{\cos\,\theta_n^t}{\mu_\perp} \tag{27}$$

for harmonics of the magnetic type, and

$$\sin\,\xi_n^t = \frac{\sin\,\theta_n^t}{\epsilon_\parallel}, \qquad \cos\,\xi_n^t = \frac{\cos\,\theta_n^t}{\epsilon_\perp} \tag{28}$$

Table 2. Same as table 1, but for cases IIC and IID.

Efficiency	s (IIC)	p (IIC)	s (IID)	p (IID)
ρ_0	0.9839	0.9125	0.9674	0.9023
τ_{-3}	0.7113×10^{-4}	0.1238×10^{-3}	0.4113×10^{-4}	0.3617×10^{-3}
τ_{-2}	0.8084×10^{-3}	0.1156×10^{-2}	0.4823×10^{-3}	0.3134×10^{-2}
τ_{-1}	0	0.3690×10^{-1}	0	0.6118×10^{-1}
τ_0	0	0	0	0
τ_1	0.1413×10^{-1}	0.4608×10^{-1}	0.3119×10^{-1}	0.3034×10^{-1}
τ_2	0.1009×10^{-2}	0.2859×10^{-2}	0.8003×10^{-3}	0.2306×10^{-2}
τ_3	0.8305×10^{-4}	0.3388×10^{-3}	0.5571×10^{-4}	0.2858×10^{-3}

for harmonics of the electric type. Thus, for refracted harmonics of the electric type, the wavevector and the ray direction are oriented either on the same side or on opposite sides of the y axis, depending on $\epsilon_\perp$ being positive or negative, respectively; whereas for refracted harmonics of the magnetic type, it is the sign of $\mu_\perp$ which determines if the two vectors are oriented either on the same side or on opposite sides of the y axis. Accordingly for case IIC, the refracted Floquet harmonics are counterposed [15] only when the incident plane wave is p-polarized; whereas counterposition occurs only for s-polarized incidence for case IID.

When $g(x) = 0\,\forall x$, total reflection takes places for cases IIC and IID for all angles of incidence and both linear polarization states. Just as for cases IIA and IIB, the diffraction efficiencies must be very carefully computed when the interface is periodically corrugated, because the number of refraction channels is infinite. Table 2 presents computed efficiencies for the same incidence conditions as in table 1, but for $\hat{c} = \hat{y}$, thereby showing that the Rayleigh method can yield convergent results for shallow gratings. However, just as in section 3.4.1, the Rayleigh method breaks down when the corrugation depth is increased.

Confining ourselves to shallow sinusoidal gratings, we computed the diffraction efficiencies as functions of θ_0 for cases IIC and IID. The plots for $h/d = 0.1$ are presented in figure 10. The specular reflection efficiencies, shown in figure 10(a), are generally high for almost all angles of incidence and for either polarization states. Rayleigh–Wood anomalies are also evident at $\theta_0 \approx 9.41$ and 39.07° in the plots. The most remarkable features of the plots in figure 10(a) are

- a sharp dip in the specularly reflected efficiency centred at $\theta_0 \approx 44^\circ$ for case IID and s-polarized incidence, and
- a blunt dip located at $\theta_0 \approx 88^\circ$ for case IIC and p-polarized incidence.

We found these two features to be associated with the resonant excitation of surface waves [44, 45].

Suppose that the corrugations are absent. For the special cases we are considering here, it is easy to show, as has been done by others for isotropic media [44, 45], that the boundary supports an s-polarized surface wave with propagation constant α_0 given by

$$\alpha_0^2 = k_0^2 \mu_\parallel \frac{\mu_\perp - \epsilon_\perp}{\mu_\perp \mu_\parallel - 1}. \tag{29}$$

Substitution of the constitutive scalars for case IID in (28) yields the value $\theta_0 = 43.80^\circ$ for exciting a surface wave. Likewise, an uncorrugated boundary supports a p-polarized surface

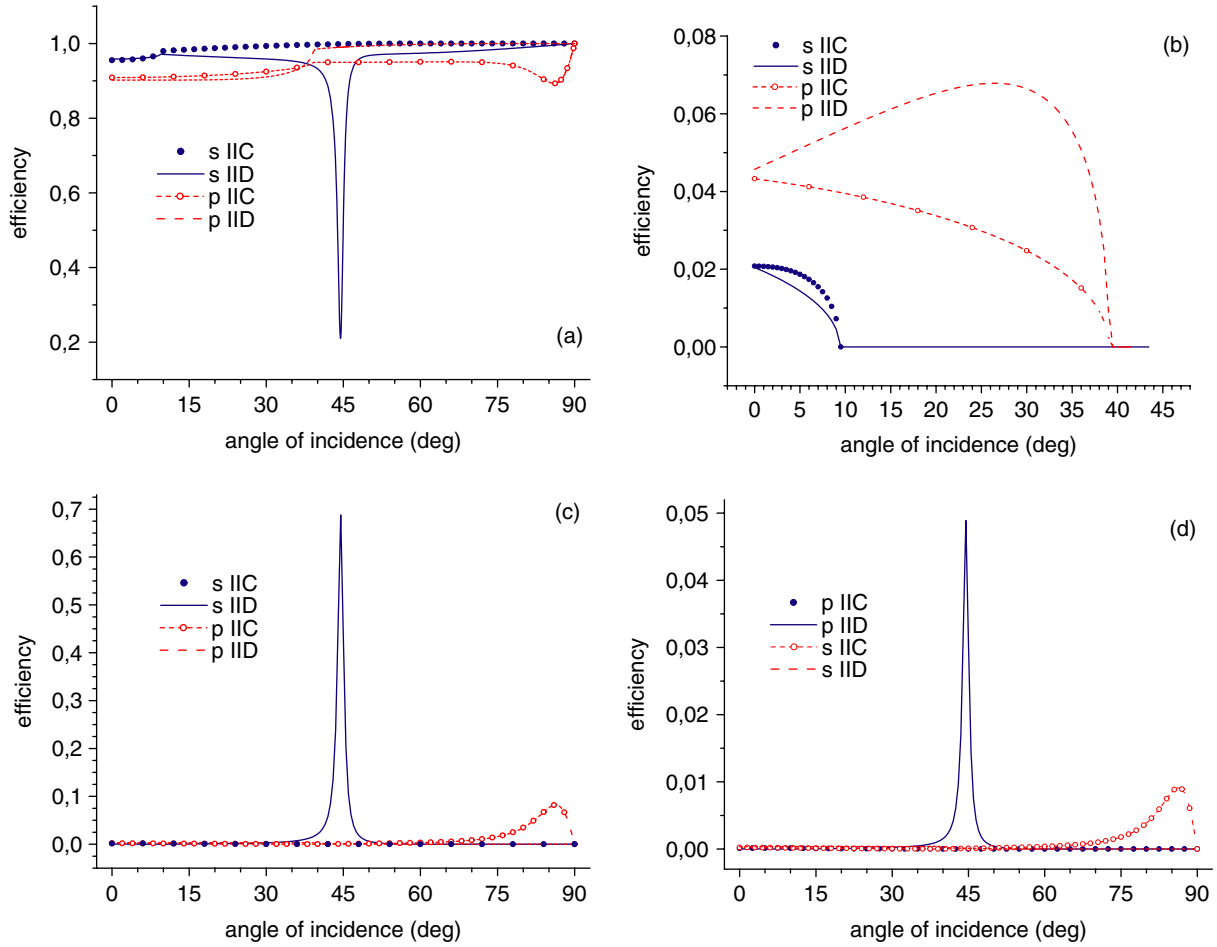

Figure 10. Diffraction efficiencies for a sinusoidal corrugation $g(x) = 0.5h \cos(2\pi x/d)$ with $h/d = 0.1$. The incident plane wave is either s- or p-polarized and the diffracting medium is described either by case IIC or IID. (a) Specular reflection ($n = 0$); non-specular refraction of order (b) $n = -1$, (c) $n = -2$ and (d) $n = -3$.

wave delineated by

$$\alpha_0^2 = k_0^2 \epsilon_\parallel \frac{\epsilon_\perp - \mu_\perp}{\epsilon_\perp \epsilon_\parallel - 1}, \tag{30}$$

and this equation yields the value $\theta_0 = 88.35^\circ$ for surface-wave excitation with the constitutive scalars chosen for case IIC. For shallow corrugations, the predictions (29) and (30) can be expected to hold approximately; and comparison with figure 10(a) indicates that our expectation is reasonable.

The resonant excitation of surface waves on gratings leaves its signature in the plots of non-specular diffraction efficiencies, as seen clearly in figures 10(c) and 10(d). For the chosen constitutive scalars, when a surface wave is excited, most of the refracted power is found in the Floquet harmonic of order $n = -2$. That would not be possible in the absence of corrugations.

4. Concluding remarks

In the foregoing sections, we considered the diffraction of plane electromagnetic waves at the periodically corrugated boundary of vacuum and a linear, homogeneous, uniaxial, dielectric–magnetic medium. To reduce the number of the many parameters involved and to be consistent with specific geometries considered previously for flat boundaries, we presented results in situations where the diffracted fields maintain the same polarization state as the s- or p-polarized incident plane wave. In the context of negative refraction, our attention was focused on two classes of media: (I) with negative-definite permittivity and permeability tensors, and (II) with indefinite permittivity and permeability tensors. For the simplest non-trivial configurations chosen for the plane wave incidence conditions and the orientation of the optic axis, the dispersion equations in the diffracting medium are elliptic for the first class of diffracting media, whereas they are hyperbolic for the second class.

By evaluating the effects of reversing signs of the eigenvalues of the relative permittivity and the relative permeability tensors of the diffracting medium, we identified instances when the grating acts either as a positively refracting interface (in the sense that the rays associated with specularly refracted Floquet harmonics bend towards the normal to the mean corrugation plane and never emerge on the same side of the normal as the incident ray) or as a negatively refracting interface (in the sense that rays associated with specularly refracted Floquet harmonics emerge on the same side of the normal to the mean corrugation plane as the incident ray).

In contrast to elliptic dispersion equations, which are commonplace for conventional gratings as well, hyperbolic dispersion equations imply the possibility of an infinite number of refraction channels. Only a small proportion of the incident power is coupled into the higher refracted orders for shallow sinusoidal gratings, a fact that ensures convergence of and the fulfilment of physical tests of the results obtained by the application of Fourier method. However, the lack of convergence observed for deeper gratings seems to be related to the existence of an infinite number of refraction channels; and we conjecture that the same problem would be experienced with other numerical techniques as well. Research will be undertaken shortly to explore different theoretical methods.

Acknowledgments

RAD acknowledges financial support from Consejo Nacional de Investigaciones Científicas y Técnicas (CONICET), Agencia Nacional de Promoción Científica y Tecnológica (ANPCYT-BID 1201/OC-AR-PICT14099) and Universidad de Buenos Aires (UBA). AL acknowledges partial support from the Penn State Materials Research Science and Engineering Center.

References

[1] Veselago V G 1968 The electrodynamics of substances with simultaneously negative values of ϵ and μ *Sov. Phys.—Usp.* **10** 509–14

[2] Lakhtakia A, McCall M W and Weiglhofer W S 2003 Negative phase-velocity mediums *Introduction to Complex Mediums for Optics and Electromagnetics* ed W S Weiglhofer and A Lakhtakia (Bellingham, WA: SPIE Press)

[3] Special issue on negative refraction 2003 *Opt. Express* **11** 639–830

[4] Pendry J B 2004 Negative refraction *Contemp. Phys.* **45** 191–202

[5] Rashed R 1990 A pioneer in anaclastics, Ibn Sahl on burning mirrors and lenses *Isis* **81** 464–91
[6] Shelby R A, Smith D R and Schultz S 2001 Experimental verification of negative index of refraction *Science* **292** 77–9
[7] Parazzoli C G, Greegor R B, Li K, Koltenbah B E C and Tanielian M 2003 Experimental verification and simulation of negative index of refraction using Snell's law *Phys. Rev. Lett.* **90** 107401
[8] Houck A A, Brock J B and Chuang I L 2003 Experimental observations of a left-handed material that obeys Snell's law *Phys. Rev. Lett.* **90** 137401
[9] Pendry J B, Holden A J, Stewart W J and Youngs I 1996 Extremely low frequency plasmons in metallic mesostructures *Phys. Rev. Lett.* **76** 4773–6
[10] Pendry J B, Holden A J and Stewart W J 1999 Magnetism from conductors and enhanced nonlinear phenomena *IEEE Trans. Micro. Theory Tech.* **47** 2075–84
[11] McCall M W, Lakhtakia A and Weiglhofer W S 2002 The negative index of refraction demystified *Eur. J. Phys.* **23** 353–9
[12] Boardman A D, King N and Velasco L 2005 Negative refraction in perspective *Electromagnetics* **25** at press
[13] Mackay T G and Lakhtakia A 2004 Plane waves with negative phase velocity in Faraday chiral mediums *Phys. Rev.* E **69** 026602
[14] Zhang Y, Fluegel B and Mascarenhas A 2003 Total negative refraction in real crystals for ballistic electrons and light *Phys. Rev. Lett.* **91** 157404
[15] Lakhtakia A and McCall M W 2004 Counterposed phase velocity and energy-transport velocity vectors in a dielectric–magnetic uniaxial medium *Optik* **115** 28–30
[16] Hu L B and Chui S T 2002 Characteristics of electromagnetic wave propagation in uniaxially anisotropic left-handed materials *Phys. Rev.* B **66** 085108
[17] Lakhtakia A and Sherwin J A 2003 Orthorhombic materials and perfect lenses *Int. J. Infrared Millim. Waves* **24** 19–23
[18] Smith D R and Schurig D 2003 Electromagnetic wave propagation in media with indefinite permittivity and permeability tensors *Phys. Rev. Lett.* **90** 077405
[19] Smith D R, Kolinko P and Schurig D 2004 Negative refraction in indefinite media *J. Opt. Soc. Am.* B **21** 1032–43
[20] Lakhtakia A 2003 On planewave remittances and Goos-Hänchen shifts of planar slabs with negative real permittivity and permeability *Electromagnetics* **23** 71–5
[21] Depine R A and Lakhtakia A 2004 Plane-wave diffraction at the periodically corrugated boundary of vacuum and a negative-phase-velocity material *Phys. Rev.* E **69** 057602
[22] Depine R A and Lakhtakia A 2004 Perturbative approach for diffraction due to a periodically corrugated boundary between vacuum and a negative phase-velocity material *Opt. Commun.* **233** 277–82
[23] Depine R A and Lakhtakia A 2005 Diffraction gratings of isotropic negative phase-velocity materials *Optik* **116** 31–43
[24] Smith D R, Rye P M, Mock J J, Vier D C and Starr A F 2004 Enhanced diffraction from a grating on the surface of a negative-index metamaterial *Phys. Rev. Lett.* **93** 137405
[25] Depine R A, Lakhtakia A and Smith D R 2005 Enhanced diffraction by a rectangular grating made of a negative phase-velocity (or negative index) material *Phys. Lett.* A **337** 155–60
[26] Lakhtakia A, Varadan V K and Varadan V V 1991 Plane waves and canonical sources in a gyroelectromagnetic uniaxial medium *Int. J. Electron.* **71** 853–61
[27] Lakhtakia A, Varadan V K and Varadan V V 1991 Reflection and transmission of plane waves at the planar interface of a general uniaxial medium and free space *J. Mod. Opt.* **38** 649–57
[28] Chen H C 1983 *Theory of Electromagnetic Waves: A Coordinate-Free Approach* (New York: McGraw-Hill) ch 1
[29] Lakhtakia A, Depine R A, Inchaussandague M E and Brudny V L 1993 Scattering by a periodically corrugated interface between free space and a gyroelectromagnetic uniaxial medium *Appl. Opt.* **32** 2765–72
[30] Lord Rayleigh 1907 On the dynamical theory of gratings *Proc. R. Soc.* A **79** 399–416

[31] Kazandjian L 1996 Rayleigh methods applied to electromagnetic scattering from gratings in general homogeneous media *Phys. Rev.* E **54** 6802–15
[32] Millar R F 1971 On the Rayleigh assumption in scattering by a periodic surface. II *Proc. Camb. Phil. Soc.* **69** 217–25
[33] Hill N R and Celli V 1978 Limits of convergence of the Rayleigh method for surface scattering *Phys. Rev.* B **17** 2478–81
[34] Popov E and Mashev L 1987 Convergence of Rayleigh–Fourier method and rigorous differential method for relief diffraction gratings: nonsinusoidal profile *J. Mod. Opt.* **34** 155–8
[35] Depine R A and Gigli M L 1994 Diffraction from corrugated gratings made with uniaxial crystals: Rayleigh methods *J. Mod. Opt.* **41** 695–715
[36] Inchaussandague M E, Gigli M L and Depine R A 2003 Reflection characteristics of a PML with a shallow corrugation *IEEE Trans. Micro. Theory Tech.* **51** 1691–5
[37] Gigli M L and Inchaussandague M E 2004 Propagation and excitation of eigenmodes at isotropic-gyroelectromagnetic index-matched interfaces *Opt. Commun.* **241** 263–70
[38] Lütkepohl H 1996 *Handbook of Matrices* (Chichester: Wiley) ch 9
[39] Lakhtakia A 2003 Handedness reversal of circular Bragg phenomenon due to negative real permittivity and permeability *Opt. Express* **11** 716–22
[40] Maystre D (ed) 1993 *Selected Papers on Diffraction Gratings* (Bellingham, WA: SPIE)
[41] Petit R (ed) 1980 *Electromagnetic Theory of Gratings* (Berlin: Springer)
[42] Born M and Wolf E 1980 *Principles of Optics* 6th edn (Oxford: Pergamon) pp 47–51
[43] Loewen E and Popov E 1997 *Diffraction Gratings and Applications* (New York: Dekker)
[44] Boardman A D (ed) 1982 *Electromagnetic Surface Modes* (New York: Wiley)
[45] Raether H 1988 *Surface Plasmons on Smooth and Rough Surfaces and on Gratings* (Heidelberg: Springer)